JME

Journal of Mining & Environment,
Vol.2, No.2, 2011, 136-145.

Relationship between fracture dip angle, aperture and fluid flow in the fractured rock masses

M. Fatehi Marji[1], A. Pashapour[2*], J. Gholamnejad[1]

1. Assoc. Prof. Faculty of Mining and Metallurgical Engineering, Yazd University, Yazd, Iran
2. Msc student in Rock Mechanics, Faculty of Mining and Metallurgy, Yazd University, Yazd, Iran

Received 25 Jan 2012; received in revised form 9 Mar 2012; accepted 5 Apr 2012
**Corresponding author: a.pashapour@stu.yazduni.ac.ir (A. Pashapour)*

Abstract
Most of the Earth's crust contains fluids, and fractures are common throughout the upper part. They exist at a wide range of scales from micro-fractures within grains to major faults and shear zones that traverse the crust. In this paper, the stress-dependent permeability in fractured rock masses have been investigated considering the effects of nonlinear normal deformation and shear dilation of fractures using a two-dimensional distinct element method program, UDEC. A new analytical and numerical model was proposed to determine the relationship between fracture dip angle, aperture and permeability. The numerical work were conducted in two ways**:** (1) increasing the overall stresses with a fixed ratio of horizontal to vertical stresses components; and (2) increasing the differential stresses (i.e., the difference between the horizontal and vertical stresses) while keeping the magnitude of vertical stress constant. The results showed that at the stress ratio of 1 the significant shear dilation occurs at an approximately low stress and mean fracture angles. For the differential stresses case, the shearing process can result in breakage of the asperities, resulting in the decrease of the dilation rate and strain softening of the fracture.

Keywords: *Stress-dependent permeability; fracture dip angle; aperture; numerical modeling; fluid flow*

1. Introduction

Modeling of fluid flow through fractured rock is important in performing the following tasks associated with fractured rock masses: characterization and development of fractured rock oil reservoirs, geothermal energy development, petroleum well design, nuclear waste repository performance assessment studies, interpretation of hydrologic tests, design of in-situ hydrologic tests, groundwater contamination studies, in-situ mine leaching studies, and stability studies of rock masses in the presence of groundwater flow. In general, fluid flow through fractured rock masses depends on the following factors: stratigraphy, fracture network pattern, flow behavior through single fracture, flow properties of matrix rock, in-situ stress system and hydraulic boundary conditions. However, the characterization of fluid flow through fractured rocks is one of the most challenging problems faced by the geotechnical engineers. This difficulty largely comes from the fact that rock is a heterogeneous material which contains various natural fractures in different scales [1]. Fractured rock masses are composed of intact rock materials and fractures, with the latter acting as the main pathways of fluid flow, especially in hard rocks. Apertures of fractures can change due to normal stress-induced closures or openings and due to shear stress-induced dilations. Hence, the permeability of fractured rock masses is stress-dependent. This process can be viewed as an 'indirect' hydro-mechanical coupling that occurs

when the applied stresses produce a change in the hydraulic properties, whereas a 'direct' coupling occurs when the applied stresses produce a change in fluid pressure and vice versa [2]. In order to understand the mechanical and hydromechanical behaviour of fractured rock masses, there is very limited number of experiments. Laboratory investigations on single rock fractures show that normal closure and shear dilation can significantly change fracture transmissivity [3, 4]. When it comes to a fracture system that contains a multitude of fractures, the changes in the transmissivities of critically oriented fractures can be much higher than that of other fractures not critically (optimally) oriented for shear failure [5]. When the shear failures and dilations of fractures are to be considered, analytical solutions do not exist. Therefore, numerical modeling has to be applied to deepen the understanding of the critical mechanisms and the contributions to the overall permeability from both normal and shear stresses [6,7]. Work by Zhang and Sanderson shows that the method of 'numerical experiment' using the distinct element code, UDEC (Universal Distinct Element Code,) is effective in the modeling fluid flow and deformation of fractured rock masses. The influence of stresses on permeability of fractured rock masses was extensively investigated considering various geometries of fracture systems [10, 11]. Such numerical experiments will be increasingly important with the advance of computing capacity due to the strength of distinct element modeling that can incorporate both hydraulic and mechanical analysis with explicit representation of fractures. The present paper focuses on the mechanical behaviour of a rock fracture under boundary stresses and their effects on the aperture on the fracture angle variation. Fractures (or joints) can be thought of as two rough surfaces in partial contact with one another, characterized by a void space between opposite walls of the fracture. When the normal stress is increased, progressive closure of the rock joint is observed, together with an increase in contact area between both walls. This evolution plays a key role in the development of flow paths through the fracture [8, 9].

2. The concept of stress at an open fracture

Hudson proposed the ISRM Suggested Method for a phenomenon which occurs naturally at an open fracture, as illustrated in Figure 1 for the 2-D case. The stress state A indicates two components of the pervasive stress state in the rock, near the fracture. States B and C, the principal stress directions are rotated and the magnitudes of the principal stresses change. In the case of an open fracture, no normal or shear stress can be sustained perpendicular and parallel to the fracture surface respectively, so the fracture surface becomes a principal stress plane with a minimum principle stress value of zero. When the fracture is partially closed or filled, the stress trajectories will be perturbed, but less severely. Imagining this effect adjacent to many fractures at all scales in a rock mass leads to the expectation that local values of in-situ stress, and site investigation measured values, are likely to be variable, possibly highly variable[12].

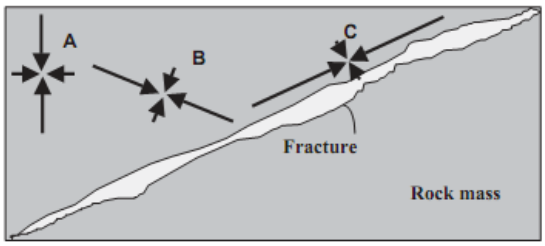

Figure. 1. An open fracture will perturb the stress field and cause the principal stresses to be locally parallel and perpedicular to the fracture surface[12].

In this study the basic mechanisms of aperture changes are illustrated resulting from two basic fracture deformations and the states of stress on fractures (figure 2). The change in fracture aperture occurs from two basic mechanisms: normal stress-induced closure or opening, and shear stress-induced dilation as shown in figure 2a. In normal stress-displacement relation, the response shows the well-known hyperbolic behaviour showing stiffer fractures with increasing compressive normal stresses. The normal deformation of a fracture is more sensitive at lower magnitudes of normal stresses. The shear dilation occurs as a result of overriding asperities of two rough fracture surfaces and may reach a stationary value with increasing fracture shearing (figure2b). Such shear dilation of fractures is of particular importance, since its magnitude can be significantly larger than the normal stress-induced closure or opening. When a multitude of fractures needs to be considered (i.e., in fractured rock masses), the fact that not all the fractures are under the same stress conditions should be properly considered (figure 2c). Firstly, the orientations of fractures play a significant role in deciding the local stress states across and along the fractures, which can be represented using the Mohr circles, as shown in figure 2d. The different stress states of fractures with different orientations, therefore, lead to different directional

hydraulic behaviour of the fractured rock masses. Secondly, when fractures have finite sizes and interact with each other, the estimation of local stress by Mohr's circle is not valid any more and detailed local stress states can only be analyzed by numerical analysis such as distinct element methods (DEM) used in this study. It is noted that the fractures modeled in this study are assumed to maintain the contact along the surfaces based on the understanding that the scale of geometric irregularity along the surface of fracture is small compared to the scale of the entire fracture. However, when there is an open fracture (with or without the fluid in it), i.e. the scale of irregularity of surface is big compared to the scale of fracture, the assumption of maintenance of contact will not be valid. When there is no fluid in the open fracture, no stress will be transmitted across the fracture and, when there is fluid in it, shear stress cannot be transmitted across the fracture.

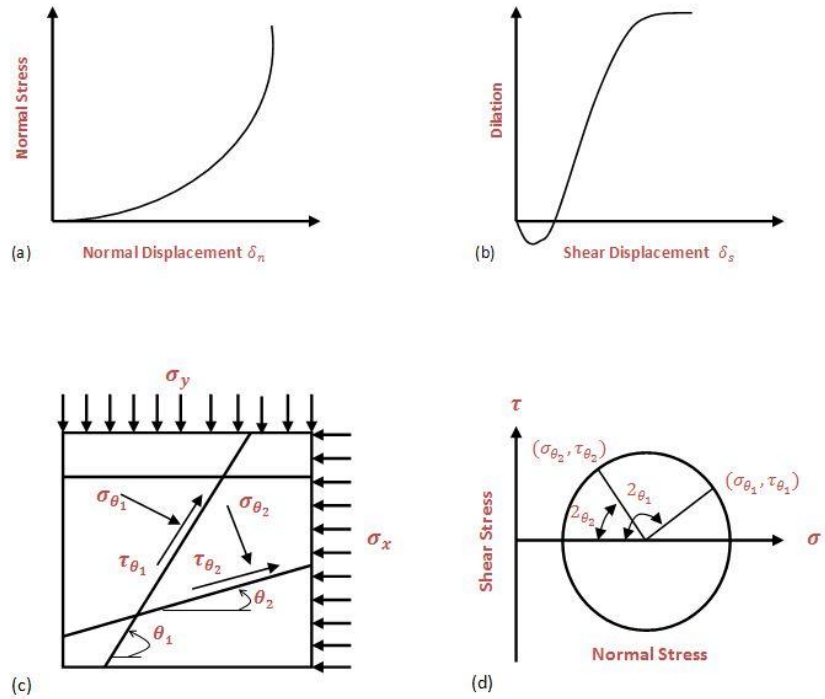

Figure. 2. Aperture changes due to two basic fracture deformations and state of stress in fractures. (a) normal stress-displacement relation, (b) shear dilation with respect to shear displacement, (c) stresses in fractures, (d) Mohr Circle (angles are measured from the horizontal line)[13]

Therefore, the stress distribution around the open fracture can be different. This aspect can be considered by more explicit representation of void shape of fractures; however, this is not the scope of this study. When the stress ratio, defined as the ratio of the maximum to minimum principal stresses in two dimensions, is too small to cause shear failure of fractures, the normal stresses will be the main source of aperture changes, leading to a general decrease of permeability of rock masses. However, when the stress ratio is large enough to cause shear failure at the critically oriented fractures, the shear dilations of these fractures can cause significant increase in their apertures, while the other less critically oriented fractures still undergo mainly normal displacements caused by normal stresses. Such non-uniformly distributed apertures may lead to changes in fracture flow paths and permeability of the region concerned. Based on this conceptualization of stress-aperture interaction in fractured rocks, the stress-loading conditions for this study are selected in two ways (figure 3). Firstly, horizontal and vertical compressive stresses are applied and increased incrementally, with a fixed ratio of horizontal to vertical boundary stresses, At K=1. It is expected that no significant shear dilation will occur under this stress condition and the effect of normal stress conditions on the overall fluid flow field and permeability of the region can be simulated. Secondly, the horizontal normal boundary stress increases incrementally while keeping the vertical normal stress constant, thus to produce increased shear stresses in the fractures, especially those with critical orientations [13]. Through this process, the impact of shear dilations of critically oriented fractures, with the resulting effect on the overall permeability, can be investigated for both pre- and post-shear failure conditions of fractures.

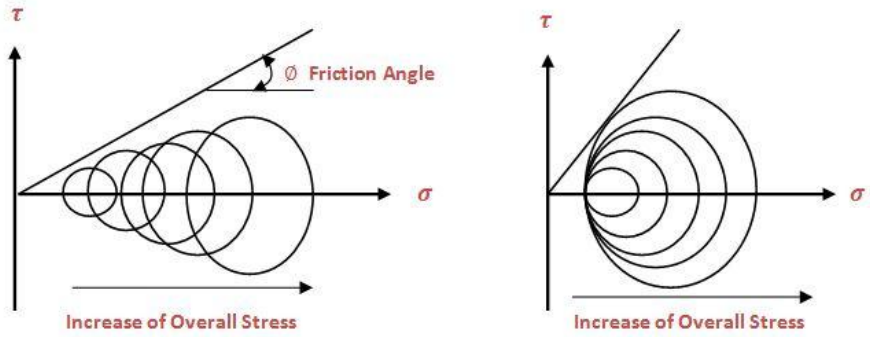

Figure.3. Two kinds of stress increase used in this study. (a) Increase of stress magnitudes while keeping the stress ratio of horizontal to vertical stress constant. (b) Increase of differential stresses while keeping the vertical, i.e. the lowest stress component, stress constant. The Mohr Coulomb failure criterion is used with the zero cohesion.

3. Procedure for analytical modeling

3.1 stress and correlate terms at the fracture

The magnitude of σ_n and τ acting on a smooth planar joint can be found from the principal biaxial stresses σ_x , σ_y acting in the mass, which yields the equations:

$$\sigma_n = \frac{1}{2}\left(\sigma_x + \sigma_y\right) + \frac{1}{2}\left(\sigma_x - \sigma_y\right)\cos 2\beta \quad (1)$$

$$\tau = \frac{1}{2}\left(\sigma_x - \sigma_y\right)\sin 2\beta \quad (2)$$

Where β is the angle between the plane on which σ_x acts and the joint plane. Barton has shown that this simple transformation can lead to substantial errors if dilation occurs during joint slippage [13]. This can be seen in figure 4, taken from Barton (1986). Biaxial tests were performed as shown in figure 4, from which it was found that the resulting stress path (1), applying equations 1 and 2, climbed above the peak strength envelope determined from full scale tilt tests. Part of this enhanced resistance was found to arise from frictional forces acting on the test platens, but correction for these still resulted in a stress path (2) climbing above the peak strength envelope. It was found that the stress path could be modified to reach the peak strength envelope (stress path 3) without violating it by including the mobilized dilation angle i_{mob} in equations 1 and 2 to give:

$$\sigma_n = \frac{1}{2}\left(\sigma_x + \sigma_y\right) + \frac{1}{2}\left(\sigma_x - \sigma_y\right)\cos 2(\beta + i_{mob}) \quad (3)$$

$$\tau = \frac{1}{2}\left(\sigma_x - \sigma_y\right)\sin 2(\beta + i_{mob}) \quad (4)$$

$$i_{mob} = \frac{1}{2}((JRC)_{mob} log_{10}(\frac{JCS}{\sigma_n}) \quad (5)$$

Where, JRC is the joint roughness coefficient and JCS is the joint shear stiffness of wall constant strength.

If the dilation angle is not included in the stress transformation the applied stresses required to cause failure may be significantly higher than estimated values. Barton also suggests that stability analyses performed in plane strain environment may give insufficient credit to the potential strength and stress changes caused by slip of non-planar joints [13].

3.2. An elastic constitutive model for rock discontinuities

To take into account the coupling between fluid flow and deformation in rock discontinuities, one can model the discontinuities by an interfacial layer, as shown in figure 5. The interfacial layer is a thin layer with complex constituents and textures (depending on the fillings, asperities and the contact area between its two opposing walls).

The apparent mechanical response of the interfacial layer can be described by Lame's constant λ and shear modulus G: As the thickness of the interfacial layer (i.e. the initial mechanical aperture of the discontinuity) is generally small compared with the size of rock matrix, it seems reasonable to assume that $\varepsilon_x = \varepsilon_y = 0$ and $\gamma_{xy} = \gamma_{yx} = 0$ within the interfacial layer.

Then according to Hook's law of elasticity, the elastic constitutive relation for the interfacial layer under normal stress σ_n and shear stress τ can be expressed in the following incremental form:

$$\begin{Bmatrix} d\sigma_n \\ d\tau \end{Bmatrix} = \begin{bmatrix} \lambda + 2G & 0 \\ 0 & G \end{bmatrix} \begin{Bmatrix} d\varepsilon_n \\ d\gamma \end{Bmatrix} \quad (6)$$

For convenience, we use u_1 to denote the relative normal displacement of the interfacial layer caused by σ_n, δ to denote the relative tangential displacement caused by τ , and u_2 to denote the relative normal displacement caused by shear dilation or shear contraction (a convention is adopted here that normal compressive displacements yields negetive values). Hence, the total normal relative displacement u is represented as:

$$u = u_1 + u_2 \quad (7)$$

Note that in Equation (7), u_2 takes positive value for dilatant shear, negetive value for contractive shear, and zero if the effect of shear dilation or shear contraction is negligible. The increments of strains, $d\varepsilon_n$ and $d\gamma$, can be expressed in terms of the increments of relative displacements, du_1 and $d\delta$, in the following form:

$$d\varepsilon_n = du_1/(b_0 - u) \quad (8)$$

$$d\gamma = d\delta/(b_0 - u) \quad (9)$$

where b_0 is the thickness of the interfacial layer or the initial mechanical aperture of the discontinuity Substituting Equation (8,9) in Equation (6) yields:

$$\begin{Bmatrix} d\sigma_n \\ d\tau \end{Bmatrix} = \begin{bmatrix} k_n & 0 \\ 0 & k_s \end{bmatrix} \begin{Bmatrix} du_1 \\ d\delta \end{Bmatrix} \quad (10)$$

where k_n and k_s denote the normal stiffness and tangential shear stiffness of the interfacial layer, respectively,

$$k_n = (\lambda + 2G)/(b_0 - u) \quad k_s = G/(b_0 - u) \quad (11)$$

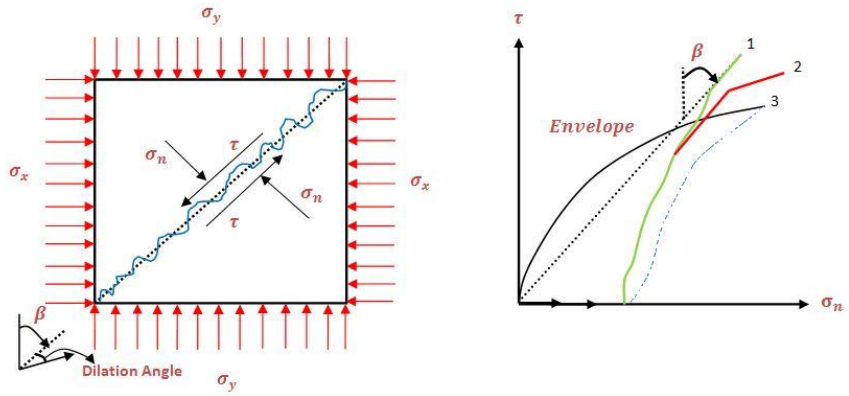

Figure .4. Biaxial stress paths on jointed rock specimen: 1, theoretical; 2, dilation corrected; 3, fully corrected. (After Barton, 1986)[13]

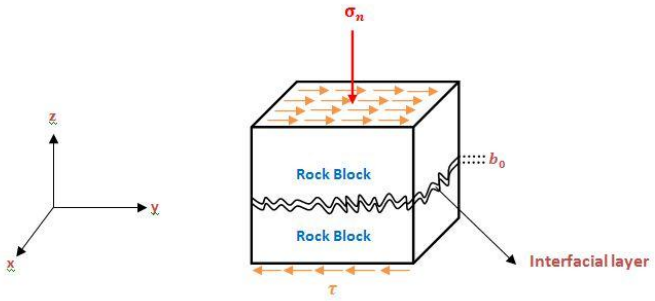

Figure 5. The interfacial layer model for discontinuities

Interestingly, k_n and k_s show a hyperbolic relationship with normal deformation and characterize the deformation response of the interfacial layer under the idealized conditions that each fracture is replaced by two smooth parallel planar plates connected by two springs with stiffness values k_n and k_s. As can be seen from Equation (11), as long as the initial normal

stiffness and shear stiffness with zero normal displacement, k_{n0} and k_{s0}, are known, they can be used as substitutes for λ and G. Substituting Equation (7) in Equation (10) results in:

$$d\sigma_n = (\lambda + 2G)\frac{du_1}{b_0 - u_1 - u_2} \quad (12)$$

$$d\tau = G\frac{d\delta}{b_0 - u_1 - u_2} \quad (13)$$

Suppose normal stress σ_n is firstly applied before the loading of shear stress, u_1 can be obtained by directly integrating Equation (12):

$$u_1 = b_0 - u_2(1 - e^{-\sigma_n/(\lambda+2G)}) \quad (14)$$

$$u_2 = b_0 - u_1\{1 - e^{(1/2G)[\arctan(|\tau|/s)-\varphi)|\tau|-(s/2)\ln 1+\tau^2/s^2\ ]}\} \quad (15)$$

Where: s is a normal stress-like parameter, and φ is a frictional angle-like parameter.

4. Procedure for numerical modeling

4.1.Model geometry and initial conditions

Figure 6 shows the simple geometrical model, which has the following features: the model consists of a seven through-going fractures, arbitrarily chosen with an angles of 0°,14°,20°,26°,31°,42°,45°,56°,72° with the X-axis one of which is separately implemented to the identifying effects of Far-field stresses on the aperture of fracture . At a small scale, this model represents most of sub-regions within a fracture network. Analyses based on the geometry of model are carried out to demonstrate the basic procedure of modelling and to examine the basic behaviour. The simulated region had an area of 10 m x 10 m. The blocks of rock between the fracture were considered to behave elastically, with parameters chosen to approximate those of a well-cemented sandstone (Table 1). The fracture was assumed to have zero cohesion, a friction angle of 35° and a dilation angle of 0 °. The hydraulic aperture of the fracture was considered to vary as a linear function of the normal stress, σ_n, as shown in figure 7 and also to be controlled by the normal displacement of the fracture given by the following equation :

$$\alpha = \alpha_0 + u_n \quad (16)$$

where α_0 is the fracture hydraulic aperture at zero normal stress; and u_n is the fracture normal displacement (positive denoting opening).

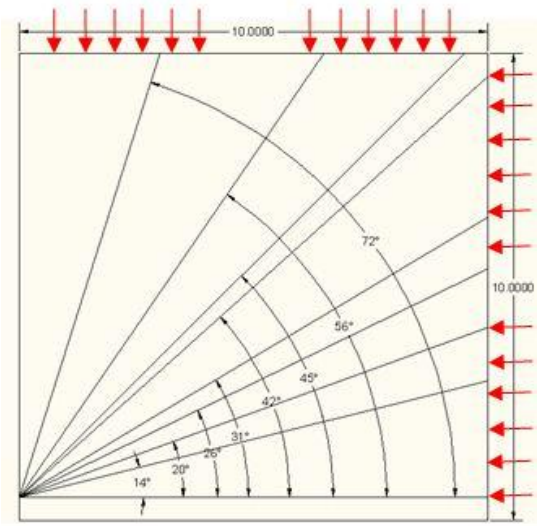

Figure 6. The simulated geometrical region with area of 10 m x 10m

4.2. Application of various stress conditions to generate deformed states of the models

After the generation of the models separately with the fracture angle aperture, various boundary stresses were applied to generate deformed models for flow analysis. The boundary stresses were selected in two ways, as described above. Each rock block between the fractures was modeled as continuous, homogeneous, isotropic, linear elastic whit an impermeable media and subdivided with a mesh of constant-strain triangle finite-difference elements. Key factors affecting the hydraulic behaviour of fractures, such as opening, closure, sliding and dilation, were modeled by incorporating relevant fracture constitutive models.

A step-wise nonlinear normal stress-normal closure relation is adopted to approximate a hyperbolic normal deformation process. The shear stress-shear displacement fracture behaviour was modeled by an elasto-perfectly plastic constitutive model with a Mohr–Coulomb failure criterion and fracture dilation occurs when it starts to slide (figure 8). This dilation continues until a pre-defined critical shear displacement ($\boldsymbol{u_{cs}}$) value beyond which the dilation stops. The necessary model parameters are listed in Table 1.

These parameters, however, were chosen to demonstrate the significance of stress-flow behavior in the model. The most important parameter for the evaluation of stress-dependent permeability is the fracture aperture value, and its

evolution with the stress-deformation paths and history. In this study, efforts were made to distinguish the hydraulic and mechanical apertures. The dilation angle is assumed to be constant irrespective of stress levels for simplicity and the model is run for 2000 time-steps, using the command "cy 2000" time-steps. A flow test was then carried out, by setting the "fluid den=1000" and "set flow steady" and by specifying flow boundary conditions "bo pp= 10e6" and "pfix pressure = 10e6".The effect of fluid pressure on the mechanical deformation was modelled by running the simulation for another 2000 time-steps using the command "cy 2000".
Then, the aperture under fluid pressure was printed out by "plot block aperture". Finally, the obtained results from the hydraulic aperture of various fracture dip angle Plotted on the charts for the sensitivity analyses (figures 9 and 10). After plotting of maximum hydraulic aperture in terms of the fracture dip angles in the two stress conditions, we can obtain prominent results from permeability of the fractures in the various dip angles. Here we present the results from incremental increase of both horizontal and vertical boundary stresses while keeping a constant stress ratio of 1. Because the stress ratio is unity, the main reason of the shear failure is not affected by stress states in most of the fractures. And also normal stress cause for the aperture change, basically closure.

Table 1 .Parameters used in the base line analysis

Model Parameters	Value	Units
Rock properties		
Density	2500	kg m^{-3}
Shear modulus	60	GPa
Bulk modulus	100	GPa
Tensile strength	0	MPa
Cohesion	0	MPa
Friction angle	0	Degree
Dilational angle	0	degree
Fracture properties		
Shear stiffness	40	$GPam^{-1}$
Normal stiffness	100	$GPam^{-1}$
Tensile strength	0	MPa
Cohesion	0	MPa
Friction angle	35	Degree
Dilation angle	0-5	Degree
Residual aperture	0.1	Mm
Zero-stress aperture	0.5	Mm

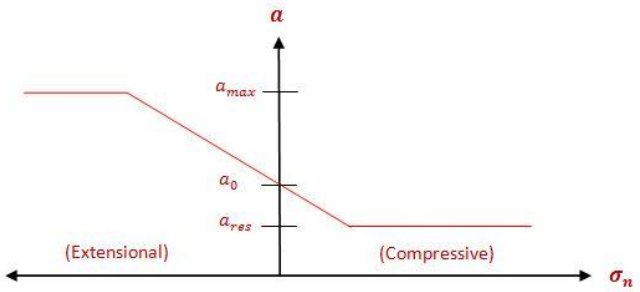

Figure 7. Relation between hydraulic aperture, a, and normal stress on fracture, $\sigma_n$in UDEC (modified from Itasca, 1996)" a_0 is zero stress aperture; a_{res} is the residual aperture; and a_{max} represents the maximum aperture

Figure 9 shows the aperture changes with the increase of boundary stresses. The initial aperture (10 mm) at a zero stress level decreased to 0.4 mm (mean values) when the mean stress magnitude was increased to 20 MPa. The changes of fracture apertures occur almost uniformly within the model region with the upturn of fracture dip angle with the increase of stresses. This is because the fracture normal closure resulting from normal stress increases is the dominating mechanism that controls fracture deformation. But at the 5 MPa stress at the angles from 14 ° unto 56°, we observed changes in the aperture, as decreasingly from the 14 ° up to 31 ° then increasingly from 31 ° up to 56°. This is because the significant shear dilation occurs at the low stress and means fracture angles. Also decreasing the aperture in angle of 56 ° up to 72 ° with k=1 at the 5 MPa stress indicating this fact (figure 9). The results show the calculated equivalent permeability change with the increases in mean stresses. Because of the dominating fracture closure with the increasing of normal stresses, the permeability of the model decreases accordingly.

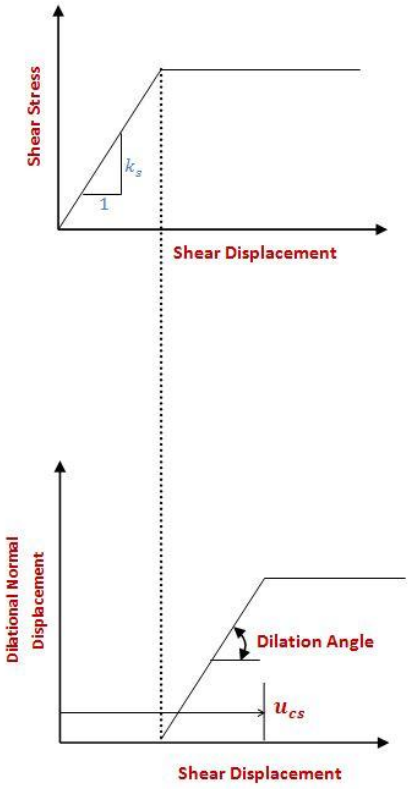

Figure 8. Shear and dilational behavior of fracture (adapted from [8]). Shear stress–displacement relation (above, fracture shear stiffness is expressed as Ks) and shear dilation–displacement relation (below).

The reduction of permeability is more than two orders of magnitude, and anisotropy in permeability is not significant, mainly because the stress ratio (k) is close to an isotropic boundary stress condition. This result is comparable to the permeability variation with the depth corresponding to stress changes [14]. Similar numerical results also showed the decrease of permeability corresponding to the increase of stresses with constant normal stiffness of fracture [15,16]. However, the application of the non-linear normal stiffness of fractures in the fracture model in this study led to more sensitive responses of permeability change at lower normal stress magnitudes, and the permeability change becomes small when the stress reaches the laboratory level of residual stress (30MPa) of fractures. This implies that permeability in shallow depth is more sensitive to that in greater depth [2]. In the next step, we present the results when the horizontal boundary stress is increased in steps from 2.5 to 25MPa, with a fixed vertical boundary stress of 5MPa (the k ratio changing from 0.5 to 5), to investigate the influence of shear failure in fractures induced by larger differential stresses. Figure 10 shows the aperture changes with the increasing stress ratio. In contrast to figure 7, fracture aperture changes are not uniform. When the stress ratio is greater than 3, prominent decrease in the aperture with the increasing fracture dip angle can be observed. An examination of the results suggests the reasons for this phenomenon and it is that mechanical degradation of these asperities occurs during shear, and the dilation of the fracture will diminish at the later stages of the shearing process, whereas Ki-Bok Mina and et al. suggest that critically-oriented fractures continue to dilate under increasing differential stresses, which leads to much larger apertures of these fractures compared to their less critically oriented neighboring fractures [18]. But our observations have not showed their results. During this process, gouge material is being produced by the damage of the asperities and the accumulation of the gouge material can result in the reduction of flow in the fracture. Plesha suggested new elastoplastic stiffness matrix of the model for this phenomenon [17]. The total increment of relative displacement at the fracture, in this case, is the sum of elastic and a plastic component; i.e.:

$$d_{u_i=}d_{u_i^e} + d_{u_i^p} \tag{17}$$

When plastic displacements occur, the asperities of the fracture are damaged, resulting in a decrease of the asperity angle. Plesha assumes that the asperity angle decreases as an exponential function of the plastic work produced by shear[20]:

$$\alpha = \alpha_0 \exp(-\int_0^{w^p} c dw^p) \tag{18}$$

where α_0 is the original asperity angle, c is a degradation coefficient, and w^p is the plastic work produced by the shear stress:

$$w^p = \int \tau du_1^p \tag{19}$$

where du_1=du is the relative joint shear displacement. From the consideration of asperity degradation, strain softening behaviour will now occur at the fracture during plastic deformation. Anisotropy of permeability emerges with the increase of differential stresses, and this anisotropy can become more prominent with the influence of shear dilation and localized flow paths.

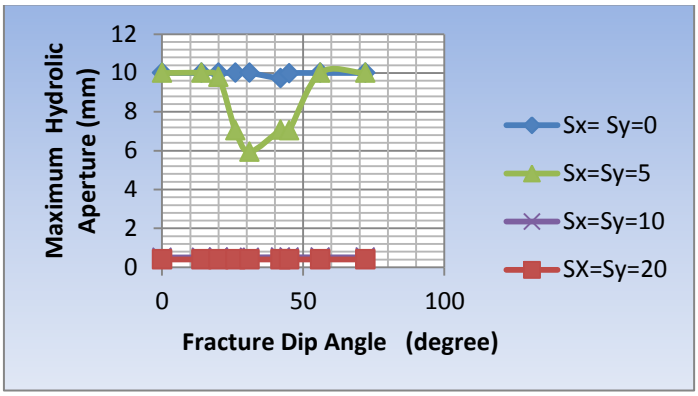

Figure 9.maximum hydraulic aperture toward variation of fracture dip angles at the various stress state with k=1

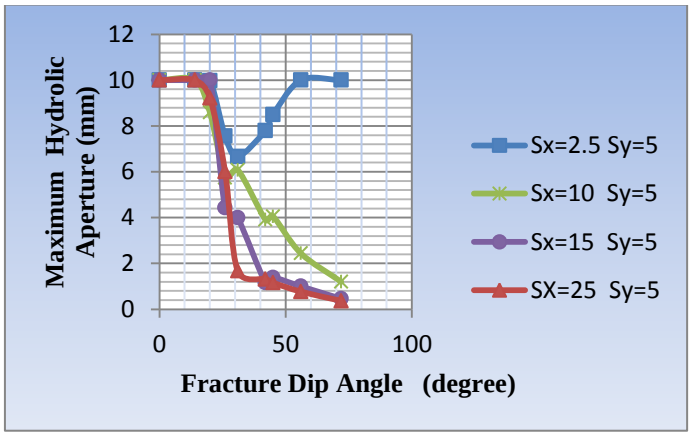

Figure.10.maximum hydraulic aperture toward variation of fracture dip angles at the differential stresses

Hence the result of our study shows a reliable behaviour of fracture orientation under differential stresses. Whereas, Ki-Bok Min et al. without spot the plastic displacements suggested that critically-oriented fractures continue to dilate under increasing differential stresses, which leads to much larger apertures of these fractures compared to their less critically oriented neighboring fractures [18]. A similar type of sudden increase of permeability atcritical stress state was shown in [11] with three types of fractured rocks. In their models, change of permeability was insensitive to differential stress before the critical stress ratio was reached because the differential stress was increased while maintaining the same mean stress. The other previous studies [15,16] did not show such sudden increase of permeability because the dilation mechanisms are not modeled. However, a limitation of the approach in this paper is the neglect of correlations between the fracture length (size) and aperture in initial model, as reported in [19]. The reason for excluding this effect are two: (1) larger fractures can always be represented as deterministic features in numerical models instead of being contributing factors to behaviour of REV that basically consider contributions from more stochastic fracture populations; and (2) lack of definite fracture length and aperture relation at the background site for the current study. However, this is an important issue since it affects different REV sizes and properties at different scales and may have significant impacts on practical applications.

5. Conclusions

In this paper, a new mathematical approach was used to estimate the aperture and permeability in the variation of fracture angle under boundary stresses for a fractured rock mass. Emphasis is placed on the coupling between fluid flow and stress/deformation, especially the effect of shear dilation or shear contraction on the hydraulic behaviour of rock fractures. Then the stress-dependent permeability of fractured rock masses is investigated through numerical experiments considering nonlinear normal deformation and shear dilation of fractures, using the distinct element method program, UDEC. While keeping a constant stress ratio of 1 between incremental increase of both horizontal and vertical boundary stresses. Because the stress ratio is unity, the stress states in most of the fractures do not cause

shear failure, and normal stress is the main cause for the aperture change, basically closure. But at the 5 MPa stress at the angles from 14° up to 56°, we observed changes in the aperture, decreasing from the 14° up to 31° then increasing from 31° up to 56°. This is because the significant shear dilation occurs at relatively low stress levels and mean fracture angles. Also, the shearing process can result in breakage of the asperities, resulting in the decrease of the dilation rate and strain softening of the fracture. It is assumed that asperity damage can be related to the plastic work of the shear stress and as a consequence the asperity angle is assumed to be a decaying exponential function of this plastic work of the shear stress at the fracture. On the other hand, gouge produced from breakage of the asperities would block the flow path and tends to decrease the joint permeability. The results of this paper confirm that high differential stresses, causing fracture shear failure at certain orientations, is one of the major reasons for highly channeled flow.
Furthermore, it may be suggested that the lengths of fractures and their connectivity may also play a dominant role in determining these major fluid-carrying features.

References

[1]. Jing L. A review of techniques, advances and outstanding issues in numerical modeling for rock mechanics and rock engineering. International Journal of Rock Mechanics and Mining Sciences 2003; 40:283–353.

[2]. Rutqvist J, Stephansson O. The role of hydromechanical coupling in fractured rock engineering. Hydrogeol J 2003;11:7–40.

[3]. Makurat A, Barton N, Rad NS, Bandis S. Joint conductivity variation due to normal and shear deformation. In: Barton N Stephansson O, editors. Proceedings of the international sympo-sium Rock Joints. Rotterdam: Balkema; 1990. p. 535–40.

[4]. Olsson R, Barton N. An improved model for hydromechanical coupling during shearing of rock joints. Int J Rock Mech Min Sci 2001;38(3):317–29.

[5]. Barton CA, Zoback MD, Moos D. Fluid flow along potentially active faults in crystalline rock. Geology 1995;23(8):683–6.

[6]. Monsen K, Makurat A, Barton N. Numerical modeling of disturbed zone phenomena at Stripa. In: Hudson JA, editor.ISRM Symposium EUROCK 92—rock characterization, 1992.p. 354–9.

[7]. Damjanac B, Fairhurst C, Brandshaug T. Numerical simulation of the effects of heating on the permeability of a jointed rock mass. Proceedings of the ninth ISRM Congress, Paris, 1999. p. 881–5.

[8]. Itasca Consulting Group. UDEC user's guide, Version 3.1, Minnesota, 2000.

[9]. Zhang X, Sanderson DJ. Numerical modelling and analysis of fluid flow and deformation of fractured rock masses. Oxford: Pergamon; 2002. 288p.

[10]. Zhang X, Sanderson DJ, Harkness RM, Last NC. Evaluation of the 2-D permeability tensor for Fractured Rock masses. Int J Rock Mech Min Sci & Geomech Abstr 1996;33(1):17–37.

[11]. Zhang X, Sanderson DJ. Effects of loading direction on localized flow in fractured rocks. In: Yuan JX, editor. Computer methods and advances in geomechanics. Rotterdam: Balkema; 1997. p.1027–32.

[12].Hudson J.A, Cornet F.H.b, Christianssonc R.ISRM Suggested Methods for rock stress estimation—Part 1:Strategy for rock stress estimation. International Journal of Rock Mechanics & Mining Sciences 40 (2003) 991–998

[13]. Parry .R H G, Mohr Circles, Stress Paths and Geotechnics. Spon Press is an imprint of the Taylor & Francis Group. © 2004. 96-97

[14]. Wei ZQ, Egger P, Descoeudres F. Permeability predictions for jointed rock masses. Int J Rock Mech Min Sci & Geomech Abstr 1995;32(3):251–61.

[15]. Zhang X, Sanderson DJ, Harkness RM, Last NC. Evaluation of the 2-D permeability tensor for Fractured Rock masses. Int J Rock Mech Min Sci & Geomech Abstr 1996;33(1):17–37.

[16]. Zhang X, Sanderson DJ. Effects of stress on the 2-D permeability tensor of natural fracture networks. Geophys J Int 1996;125:912–24.

[17]. M. E. Plesha, 'Constitutive models for rock discontinuities with dilatancy and surface degradation', Int. J. Nume Analyt. Meth. Geomech., 11, 345Ð362 (1987).

[18]. Mina K.B, Rutqvist J, Tsang C.F, Lanru J. Stress-dependent permeability of fractured rock masses: a numerical study. International Journal of Rock Mechanics & Mining Sciences 41 (2004) 1191–1210.

[19]. Ito T, Swenson D, Hayashi K. Effect of thermal deformation on fracture permeability in stressed rock masses. In: Stephansson O,Hudson JA, Jing L, editors. International Conference on Coupled T-H-M-C Processes in Geosystems: GeoProc 2003. Stockholm,2003. p. 671–76.

[20]. Plesha M. E. Constitutive models for rock discontinuities with dilatancy and surface degradationÕ, Int. J. Numer. Analyt. Meth. Geomech., 11, 345Ð362 (1987).